NASA Technical Memorandum 89056

DYNAMIC ANALYSIS OF THE LARGE DEPLOYABLE REFLECTOR

Robert E. Calleson
A. Don Scott

January 1987

(NASA-TM-89056) DYNAMIC ANALYSIS OF THE LARGE DEPLOYABLE REFLECTOR (NASA) 34 p CSCL 22B
N87-16050
Unclas
G3/18 43371

National Aeronautics and
Space Administration

Langley Research Center
Hampton, Virginia 23665

DYNAMIC ANALYSIS OF THE LARGE DEPLOYABLE REFLECTOR

SUMMARY

The Large Deployable Reflector (LDR), an astronomical observatory in low-Earth orbit, will operate above the Earth's obscuring atmosphere and perform studies in the spectral range at wavelengths of 30 to 1,000 um. Current planning projects an LDR flight in the mid-1990's.

The dynamic analysis of two proposed LDR concepts has been conducted. Response from chopping and slew excitations was obtained for two 20-meter LDR concepts. One concept was developed by NASA Ames Research Center and utilized two secondary mirror module support configurations (six strut and triple bipod); the other by NASA Jet Propulsion Laboratory utilized a stiff-mast mirror support. Chopping, a forced oscillation of the secondary mirror for the purpose of subtracting background signals from target signals, was applied to the Ames concept. The excitation from slew, a pointing manuever, was applied to both concepts. Chopping excitations caused module rotation to exceed the 0.02-arc-second requirement in the Ames six-strut configuration, but module rotation in the triple-bipod configuration was two orders of magnitude less. Response of the primary mirror from slewing in all configurations was predominantly from reflector rocking relative to the spacecraft. An increase in the damping ratio from 0.002 to 0.02 reduced the rocking amplitudes to a level less than the 0.02-arc-second requirement within the required 1-minute maximum settling time.

INTRODUCTION

The Large Deployable Reflector (LDR) is to be an astronomical observatory orbiting above the Earth's obscuring atmosphere and operating in the spectral range at wavelengths between 30 and 1,000 um. The LDR will be used to study such astronomical phenomena as stellar and galactic formations, cosmology, and planetary atmospheres. With the current state of technology, the LDR will be ready in the mid-1990's.

The LDR will represent a significant change in past observatory design and philosophy. The LDR will be the first observatory to be erected and assembled in space. This distinction brings with it several major technological challenges such as the development of ultra-lightweight deployable mirrors, advanced mirror fabrication techniques, advanced structures, and control of vibrations due to various sources of excitation. The purpose of this analysis is to provide preliminary information about the extent of vibrational response due to secondary mirror chopping and LDR slew.

The dynamic response of two 20-meter LDR configurations was studied. The first concept was developed by NASA Ames Research Center, the second by NASA Jet Propulsion Laboratory. Two mirror support configurations were investigated for the Ames concept. The first employs a six-strut secondary mirror support structure, whereas the second uses a triple-bipod-support design. All three configurations were modeled using a tetrahedral truss design for the primary mirror support structure. Response resulting from secondary mirror chopping was obtained for the two Ames configurations, and response of the primary mirror from slewing was obtained for all three configurations. The following sections discuss the LDR requirements and structural modeling as well as the modal and response analyses and results.

DISCUSSION

LDR Requirements

LDR performance requirements relevant to this study were selected from references 1 and 2 and are listed in table 1. A diameter of 20 meters, an F/ratio of 0.7, and an assumed parabolic surface determine the size and shape of the primary mirror tetrahedral truss support structure. The secondary mirror diameter of 1.3 meters is only applicable to the Ames configuration. The JPL configuration involves the passive primary, secondary, and tertiary mirrors and an active quaternary mirror--the latter three mirrors being supported in a relatively stiff mast.

The absolute pointing requirement is included here for information but is not involved in the dynamic analysis, as it is considered to be a control system requirement for the LDR as a rigid body. Jitter, however, is the dynamic response of the elastic LDR resulting from slew, scan, or track. Of these three maneuvers, the slew maneuver requires orders of magnitude more control torque and hence is the maneuver related to the jitter limitation of 0.02 arc seconds allowing 1 minute of settling time. Slewing the LDR 90° at an average rate of 45°/minute establishes parameters for the torque profile.

The purpose of chopping is to subtract background signals from the star signals. It is accomplished by chopping or oscillating the secondary mirror at 2 Hz with an approximate square wave having a throw or double amplitude of 1 arc minute. The system is assumed to be 99 percent reactionless that the actuated torques are counterbalanced in a way which prevents reactions on the module support struts leaving 1 percent of the actuated torque to excite secondary mirror module jitter.

LDR Models

The JPL and Ames concepts illustrated in figures 1 and 2 provided the basis for the three configurations. The two versions of the Ames concept differ only in the secondary mirror module support strut design. References 1 and 2 provided applicable information for developing the three finite element models shown in figures 3-5. Note that the figures include only those model grid numbers referred to in the discussion. The primary mirror truss model shown in figure 6 is a tetrahedral truss design that is common to the three configurations. This truss was modeled by the Interactive Design and Evaluation of Advanced Spacecraft (IDEAS) program of reference 3. All structural members were assumed to be fabricated with graphite/epoxy composite material with a modulus of elasticity of 130.3 GPa. Material density for all finite elements, except those representing the shade elements, the spacecraft modules, and the secondary mirror module, is 1661 kg/m^3. Shade element densities for the Ames and JPL concepts are 7428 kg/m^3 and 4813 kg/m^3, respectively. These are fictitious densities calculated to reflect the sunshade areal density of 0.645 kg/m^2 given in reference 2. Zero densities were assumed for the modules and were replaced with nonstructural mass. Member sizes and component weights are summarized in tables 2 and 3, respectively. Where sizes and weights were not available in references 1 and 2, appropriate values were assumed.

The spacecraft is composed of two modules: the resource module starting at point 110 (figure 3) and the support module which is assumed to end at point 31 in the upper surface of the primary mirror truss (figure 6). The instrument module and optical system concatenate with the spacecraft with the optical system ending at point 134 shown in figure 3. Construction of the Ames models is similar except that there is no optical system and the instrument module terminates at point 31.

To simplify the shade modeling and reduce the number of shade modes of vibration, the shade is modeled with one frame in the JPL model and two frames in the Ames model. Frame members are modeled as beam elements to provide shade stability, and the remaining members are axial elements.

The primary mirror is comprised of many individual segments. The number of segments varies with the mirror concept. There is also a wide variation of mirror segment weights reflecting choice of materials, structural design, method of support, and segment size. References 1 and 2 indicate areal density varying from 5 to over 50 kg/m^2. An arbitrary weight of 20 kg/m^2 was chosen for this analysis. This was uniformly distributed in the model by locating equal point masses at the upper surface truss grid points.

A summary of the LDR mass and moments of inertia for the completed models is given in table 4. The inertias were used in determining the required torques for the slew maneuvers.

Modal Analysis

Modal frequencies and mode shapes were determined by using the eigenvalue/eigenvector determination technique. This method calculates the eigenvalues and eigenvectors starting with the assumption of undamped free vibration giving the equation of motion,

$$Mx + Kx = 0 \tag{1}$$

and the resulting eigenvalue/eigenvector equation,

$$K\phi = \omega^2 M\phi \tag{2}$$

where K and M are, respectively, the global stiffness and mass matrices associated with the finite element model. The symbols ω^2 and ϕ are, respectively, the matrices of the eigenvalues and eigenvectors, or modal frequencies squared and mode shapes, associated with the free vibration of the model. Two finite element programs were used in developing and solving equation (2): the Interactive Design and Evaluation of Advanced Spacecraft (IDEAS), (ref. 3), and the Engineering Analysis Language (EAL), (ref. 4). IDEAS expedited the development of the tetrahedral truss--the geometry for which was transferred to EAL. Modal solutions from both programs provided confirmation of results. The documented results were determined by the EAL program.

Modal frequencies for the first 25 modes of each configuration are given in tables 5-7 for the JPL, Ames six-strut, and Ames triple bipod strut configurations, respectively. As the LDR models are free from any support constraints, as in space, the first six modes are rigid body modes with zero frequencies. The remaining modes are flexible body modes, and of these the most significant in this analysis are modes involving primary reflector rocking and secondary mirror module motion.

Selected mode shapes are shown in figures 7-30 for the three configurations. The reflector rocking modes are shown in figures 7, 15, and 24. Note that in all the mode shape figures, for clarity only the upper surface tetrahedral truss members are plotted. Secondary mirror module rotation is shown in the 11th mode, figure 18, for the six-strut configuration, but this rotation is not obvious in modes for the triple-bipod configuration. Module translation but not rotation is apparent in mode 21, figure 27; however, examination of the eigenvector output shows rotation as well. Some of this rotation is from reflector rocking. The presence of module rotation will be shown in the discussion of response.

Forcing Functions

In the examination of jitter response, two forcing functions or excitations were applied to the LDR models. One is from chopping of the secondary mirror in the Ames configurations (fig. 31), and the other is from slewing or rotation of the LDR to a desired position (fig. 32).

Chopping.- Application of the requirements for secondary mirror chopping involved the following assumptions. The 2-Hz "square" wave was modified to include a rise time of 10 percent. The 1-arc-minute throw is a double-amplitude rotational displacement of the secondary mirror with the zero displacement position ($\theta = 0$) located at one of the mirror stops. The "reactionless" system is such that the mirror inertial torque is counterbalanced in a manner that is 99 percent contained; the remaining 1 percent is reacted by the LDR structure. In other words, only 1 percent of the calculated torque acting on the mirror is used as an excitation.

Reference 2 describes the secondary mirror assembly or module as being 3 meters in height, 1.3 meters in diameter, and supported by triple-bipod struts or six struts as shown in figure 31(a). Included are module moments of inertia based on an assumed 1000-kg solid cylinder. These were included in the model for the modal analysis as a concentrated mass at points 115 and 113 as shown in figures 4 and 5. For the 200-kg mass as given in reference 2, the mirror moment of inertia (I) is calculated as 21.13 kg-m^2 by assuming a solid disk with a diameter of 1.3 meters.

A 10-percent rise time in a 2-Hz displacement square wave requires the assumption of a 0.025-second pulse of torque every 0.25 second as shown in figure 31(b). The magnitude of the torque (T) must equal the product of the mirror mass moment of inertia (I) and angular acceleration ($\ddot{\theta}$), $T = I\ddot{\theta}$. Integration leads to $\theta = Tt^2/2I$. Since T is a constant and θ is a maximum (θ_{max} = 1 arc min) at t = 0.025 second,

$$\theta_{max} = Tt^2/2I = 1 \text{ arc min} = 0.291\text{E-}03 \text{ rad}$$

and

$$T = 0.931I$$

As previously shown, I = 21.13 kg-m^2. Therefore, T = ±19.67 N-m (±174 in-lb). For a 99 percent reactionless system, T = ±0.197 N-m (±1.74 in-lb). This excitation torque was applied at point 115 in figure 4 and point 113 in figure 5 for the two Ames configurations.

Slew maneuver.- This analysis assumes the same condition considered by JPL in reference 1; that is, a total slew angle of 90° is assumed complete in 2 minutes, which complies with the requirement. The control torque, accomplished with control moment gyros (CMG), is assumed to vary as a versine function (fig. 32). The torque profile is defined as follows:

$$T = A(1 - \cos wt) \qquad 0 < t < 60 \text{ sec}$$

$$T = -A(1 - \cos wt) \qquad 60 < t < 120 \text{ sec}$$

where w equals $2\pi/120$ rad/sec and A is a constant to be determined for each configuration. The torque (T) must also equal the product of the mass moment of inertia (I) and the angular acceleration (θ). Equating $I\theta$ to each of the above expressions for T yields differential equations which can be integrated to yield the following equations for the slew position or angle, θ:

$$\theta = \frac{A}{I}\left[\frac{t^2}{2} - \frac{3600}{\pi^2}\left(1-\cos\frac{\pi}{60}t\right)\right] \qquad 0 < t < 60 \text{ sec}$$

$$\theta = -\frac{A}{I}\left[\frac{t^2}{2} - 120t + 3600 + \frac{3600}{\pi^2}\left(1-\cos\frac{\pi}{60}t\right)\right] \qquad 60 < t < 120 \text{ sec}$$

By substituting $t = 120$ sec and $\theta = \pi/2$ in the second equation for θ, the maximum torque (2A) for each configuration (see fig. 32) is determined as $T_{max} = 2A = \pi I/3600$. In addition to the torque profile and slew position, figure 32 includes a summary of T_{max} for the three LDR configurations. The respective torque profiles were applied at points 115, 112, and 111 about the y-axes of the models shown in figures 3, 4, and 5.

Response

The dynamic response of the various LDR models depends on the results of the modal analysis, internal damping, and the external forces. The following equations define the dynamic response of the models:

$$\ddot{q} + 2z\omega q + \omega^2 q = \phi^T f \qquad (3)$$

$$y = \phi q \qquad (4)$$

where z, ω, q, ϕ, f, and y are the matrices of the viscous structural damping ratios, modal frequencies, generalized displacements, mode shapes, forcing function and true nodal displacements, respectively. The external force or forcing function is applied at the desired nodal location. The structural damping ratios, which vary with the modal frequencies, currently can only be determined through experimentation. Therefore, the damping ratio was assumed to be contant throughout the modal frequency range.

Response analysis determined with the EAL program (ref. 4), is limited to the response of the secondary mirror module due to chopping and to the response of the primary reflector due to slewing. Two sets of results are given: one for the 0.002 damping ratio and another for the 0.02 damping ratio. Jitter displacements at significant points in time for the three configurations are given in table 8. Displacement time histories are shown in figures 33 through 37.

Chopping.- Response is limited to the two Ames configurations which differ only in the way the secondary mirror module is supported. The six-strut configuration exhibits orders of magnitude greater module rotation than the triple-bipod-strut configuration (table 8) because the centerlines of the six struts intersect at the module center of mass, and provide resistance to rotation only through strut bending and twist. The triple-bipod-strut design provides a much stiffer resistance through strut axial stiffness, as is normally found in a truss. As a result, the six-strut configuration exceeds the requirement of 0.02 arc second by an order of magnitude, whereas the bipod configuration exhibits module rotation two orders of magnitude less than the requirement.

Examination of the response shown in figures 33 and 34 for both configurations shows that the higher damping significantly reduces the time required for the transient vibration to damp out. The remaining steady state or forcing vibration amplitude is over half of the maximum, but still much too high in the six-strut configuration. In the triple-bipod configuration, the amplitudes with both levels of damping are almost insignificant. In this case, the determining factor in meeting the requirement was not an increase in damping, but rather one of structural configuration.

Slew.- The response of the primary reflector from slewing in all three configurations is predominantly from reflector rocking which can be seen in the seventh mode (figs. 7 and 15) of the first two configurations and the ninth mode (fig. 24) of the triple-bipod-strut configuration. These are the first and third elastic modes, respectively. Because of the structural similarity of the three configurations, it is not surprising to see the similarity in responses shown in table 8 and figures 35 through 37. The effect of increasing the damping ratio one order of magnitude to 0.02 clearly (see table 8) brings the reflector pointing deviations to well within the requirement of 0.02 arc second 1 minute after slew.

CONCLUSIONS

Jitter response of three large deployable reflector (LDR) configurations was examined. Two forms of excitation were applied. One is from chopping or oscillation of the secondary mirror for the purpose of subtracting background signals from star signals. The other is from slewing the LDR to a desired position.

Because of insufficient definition of the JPL optical system, chopping response is limited to two Ames configurations which differ only in the way the secondary mirror module is supported. Module rotation in the six-strut configuration exceeds the 0.02-arc-sec requirement by an order of magnitude, but module rotation in the triple-bipod configuration is two orders of magnitude less than the requirement. Damping is required to decay transient vibrations. In this case, the determining factor in meeting the requirement was not an increase in damping, but rather the structural configuration.

The response of the primary mirror from slewing in all three configurations is predominantly from reflector rocking relative to the spacecraft. The similar response is primarily the result of similarity in the models and mass distribution. The order of magnitude increase in damping ratio to 0.02 reduced the rocking amplitudes to less than the requirement of 0.02 arc sec within the required 1 minute maximum settling time. As 0.02 is considered relatively high internal structural damping, some additional form of damping or active control may be required.

REFERENCES

1. Swanson, Paul N., "A Lightweight Low Cost Large Deployable Reflector (LDR), A Concept Study by the Jet Propulsion Laboratory," JPL D-2283, June 1985.

2. NASA Ames Research Center, "Large Deployable Reflector (LDR) Systems Concept and Technology Delimition Study," GP-00865, Volumes I, dated March 15, 1985 and Volume II, dated February 28, 1985.

3. Garrett, L. Bernard, "Interactive Design of Future Large Spacecraft Concepts," NASA TP-1937, December 1981.

4. Whetstone, W. D., "E1SI-EAL Engineering Analysis Language Reference Manual," Engineering Information Systems, Incorporated, July 1983.

TABLE 1. - SELECTED LDR PERFORMANCE REQUIREMENTS FOR DYNAMIC ANALYSIS

Parameters	*Requirements
Diameter	20 m primary, 1.3 m secondary
F/ratio	F/0.7 primary
Absolute pointing	0.05 arc sec
Jitter	0.02 arc sec - within 1 min after slew
Slew	20° - 50°/min
Scan	1°×1° - linear scan at 1°/min
Track	0.2°/hour (for comets ≥ 25° from Sun)
Chopping	2 Hz square wave, 1 arc min throw (reactionless)

*Selected from reference 1.

TABLE 2. - STRUCTURAL MEMBER SIZES

Tubular Components	Tube Diameter (mm)	Tube Thickness (mm)	Length (mm)	
			JPL	AMES
Resource module	4500	2.0	6600	(2)
Support module	4500	2.0	3000	(2)
Instr. module	4500	2.0	6800	(2)
Optical system (1)	3800 max	2.0	7000	—
	1100 min	2.0		
Primary mirror truss				
Upper surface	39.4	0.66	2956	2956
Diagonals	28.2	0.66	1744	1744
Lower surface	39.4	0.66	2934	2934
Shade				
Frames	152.4	0.66	11582	11582
Diagonals	78.4	0.66	12629	11123 upr 9927 lwr
Verticals	78.4	0.66	12292	9496

(1) For JPL model.
(2) Total length of Ames modules assumed to be 9910 mm.

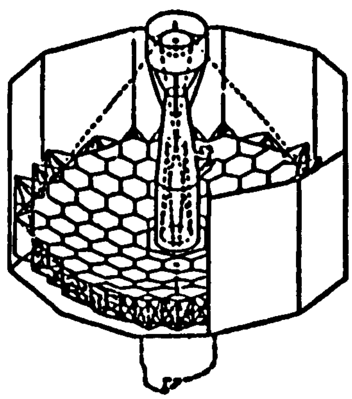

Figure 1. - JPL Concept

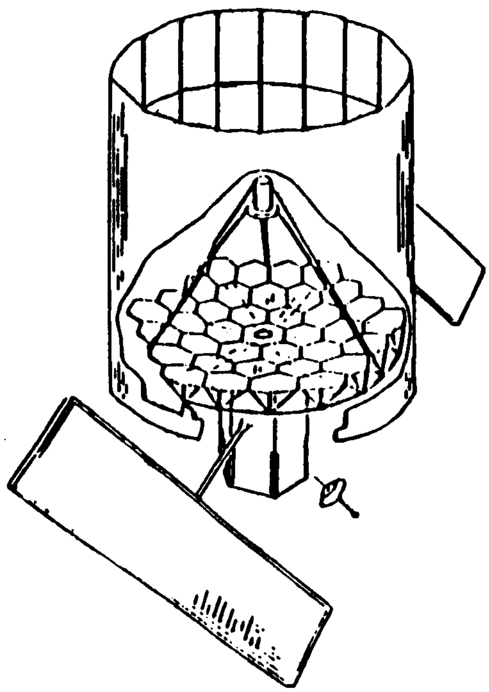

Figure 2. - Ames Concept

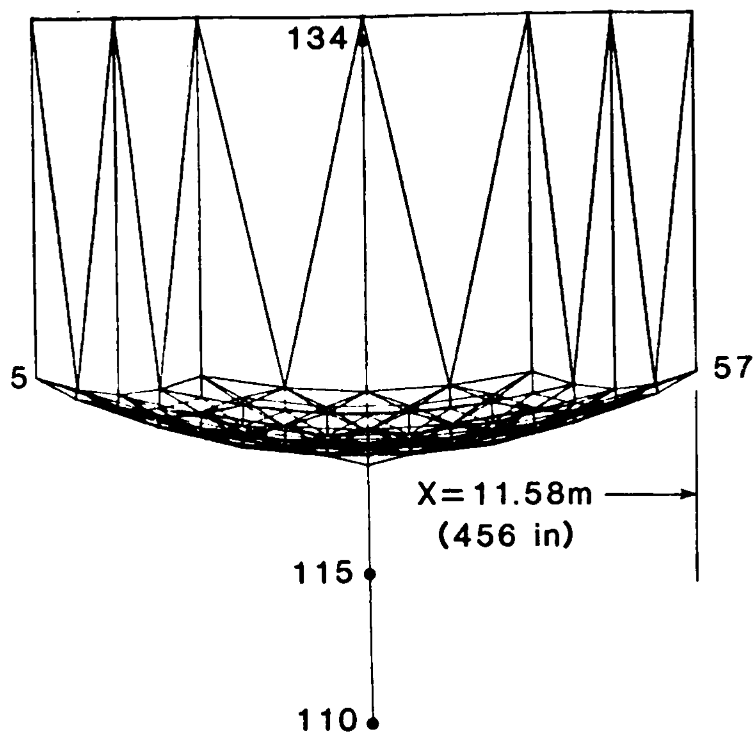

Figure 3. - JPL Model

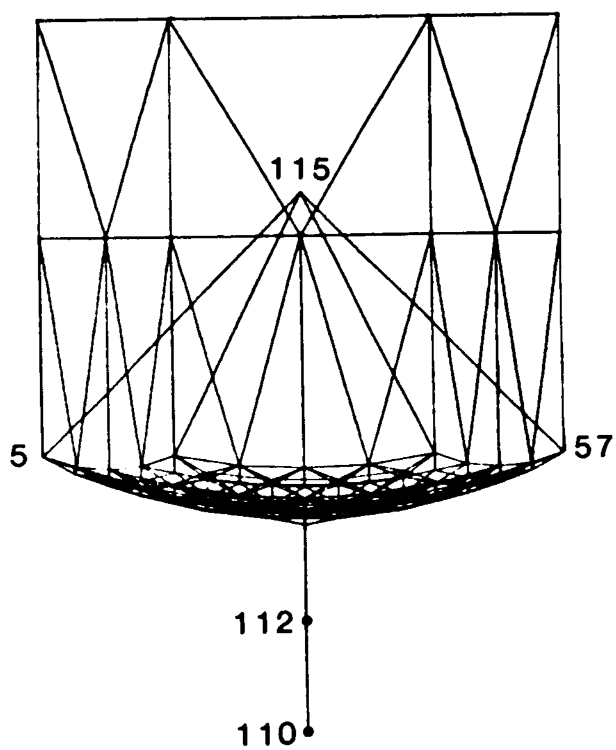

Figure 4. - Ames Six-Strut Model

ORIGINAL PAGE IS
OF POOR QUALITY

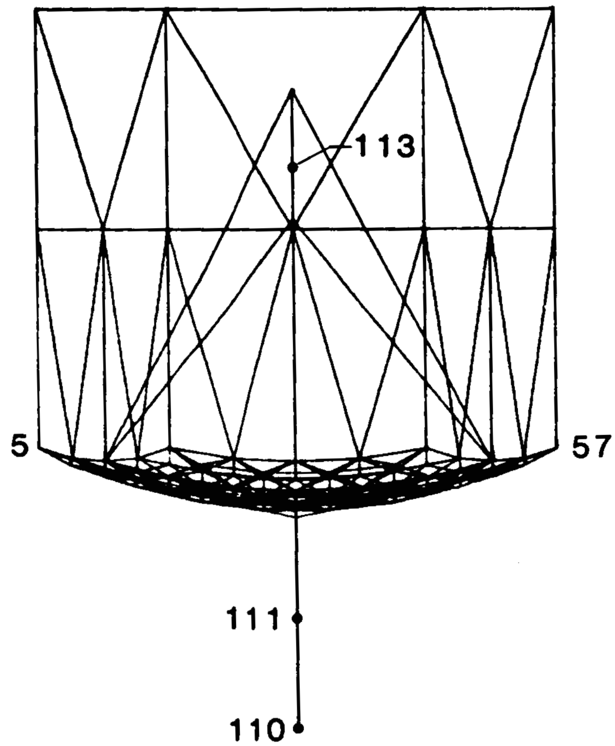

Figure 5. - Ames Triple-Bipod Strut Model

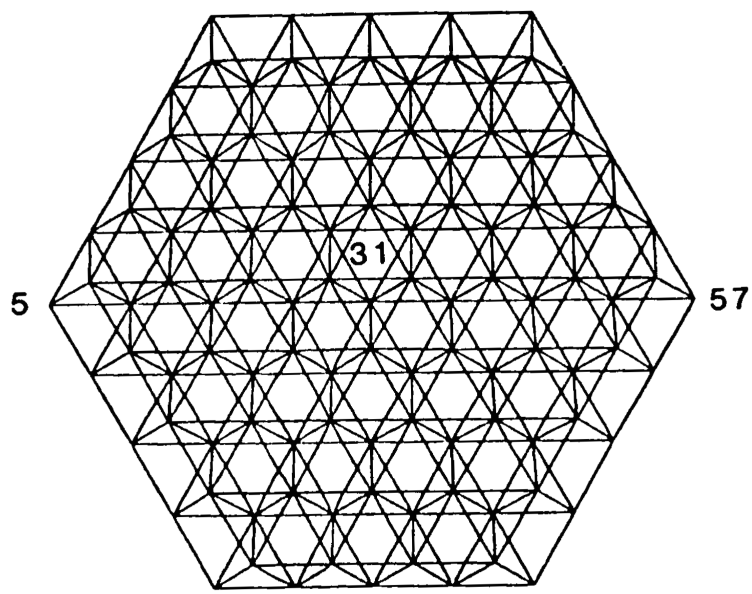

Figure 6. - Primary Mirror Truss

Table 3.- LDR COMPONENT WEIGHTS (kg)

Component	AMES	JPL	Distribution
Modules	Total is		
Resource module	uniformly	7999	Uniform over 6.6 m
Support module	distributed	1237	Uniform over 3.0 m
Instrument module	over 9.91m	3393	Uniform over 6.8 m
Total	10000	12628	
Primary mirror (20 kg/m^2)	9124	9124	Concentrated masses on truss upper surface joints
Secondary mirror module	1000	———	Concentrated mass
Optical systems less primary	———	1126	Uniform over 7.0 m
Primary mirror truss	136	136	Uniform
Secondary mirror struts	51	———	Uniform
Sunshade (.645 kg/m^2)	998	463	Reflected in fictitious material density
Total	21309	23477	

TABLE 4. - LDR MASS AND INERTIA PROPERTIES

Configuration	Mass (kg)	Moments of Inertia (kg·m^2) Ix	Iy	Iz
JPL	23477	939,000	939,000	701,000
AMES six strut	21309	1,130,000	1,130,000	770,000
AMES triple bipod	21309	1,155,000	1,155,000	769,000

Note: Products of inertia are small.

TABLE 5. - JPL MODAL FREQUENCIES (Hz)

Mode	Freq	
1	.00	Rigid body
2	.00	Rigid body
3	.00	Rigid body
4	.00	Rigid body
5	.00	Rigid body
6	.00	Rigid body
7	.54	Reflector rocking plus shade motion
8	.54	Same
9	.61	Shade frame motion
10	.61	Same
11	1.34	Same
12	1.54	Symmetrical reflection motion
13	1.97	Shade motion
14	2.73	Same
15	2.73	Same
16	3.27	Unsymmetrical reflector motion plus shade motion
17	3.27	Same
18	3.31	Symmetrical reflector motion
19	3.61	Unsymmetrical reflector motion plus shade motion
20	3.61	Same
21	3.74	Unsymmetrical reflector motion plus shade motion
22	3.74	Same
23	3.93	Shade motion
24	3.95	Unsymmetrical reflector motion plus shade motion
25	4.41	Same

TABLE 6. - AMES SIX-STRUT MODAL FREQUENCIES (Hz)

Mode	Freq	
1	.00	Rigid body
2	.00	Rigid body
3	.00	Rigid body
4	.00	Rigid body
5	.00	Rigid body
6	.00	Rigid body
7	.68	Reflector rocking plus shade motion
8	.68	Same
9	1.43	Shade frame motion
10	1.47	Symmetrical reflector motion
11	1.52	Sec. mirror assy. rot. about y axis
12	1.52	Sec. mirror assy. rot about x axis
13	1.72	Shade frame motion
14	1.74	Shade frame motion
15	2.12	Sec. mirror assy. rot. about z axis
16	2.51	Shade frame motion
17	2.51	Same
18	2.54	Same
19	2.77	Same
20	2.81	Same
21	2.85	Same
22	3.01	Symmetrical reflector motion
23	3.09	Unsymmetrical reflector and shade motion
24	3.09	Same
25	3.75	Same

TABLE 7. - AMES TRIPLE-BIPOD MODAL FREQUENCIES (Hz)

Mode	Freq	
1	.00	Rigid body
2	.00	Rigid body
3	.00	Rigid body
4	.00	Rigid body
5	.00	Rigid body
6	.00	Rigid body
7	.55	Shade frame motion
8	.56	Shade frame motion
9	.65	Spacecraft module rocking rel. to reflector
10	.65	Spacecraft module rocking rel. to reflector
11	1.17	Shade frame motion
12	1.43	Shade frame motion
13	1.48	Sym. reflector motion
14	1.89	Shade frame motion
15	1.90	Shade frame motion
16	1.94	Strut motion
17	2.51	Shade frame motion
18	2.51	Shade frame motion
19	2.85	Shade frame motion
20	2.98	Reflector, strut & secondary mirror assy motion
21	2.98	Reflector, strut & secondary mirror assy motion
22	3.04	Sym. reflector motion
23	3.59	Unsym. reflector & strut motion
24	3.59	Unsym. reflector & strut motion
25	3.74	Strut motion

TABLE 8. - JITTER DISPLACEMENTS DUE TO CHOPPING & SLEW

LDR Configuration	Damping ratio	Jitter (1)		
		Chopping (2)	Slew (3)	
		$\widehat{\text{sec}}$	Δ (microns)	Φ ($\widehat{\text{sec}}$)
JPL	.002	———	838.200	14.9
	.020	———	0.508	.0090
Ames six strut	.002	.205 (4)	685.800	12.2
	.020	.120 (5)	0.211	.0038
Ames triple bipod	.002	.000069 (4)	787.400	14.0
	.020	.000059 (5)	0.122	.0022

Comments:

(1) Requirement $\leq$ .02 $\widehat{\text{sec}}$.

(2) Secondary mirror module rotation response from secondary mirror chopping.

(3) Δ = reflector truss edge displacements (z) at point 57 (see fig. 3-5) 1 min. after slew maneuver (t~180 sec.). Based on slew of 90° in 2 min. with 1 min. settling time.
Φ = rotation of reflector truss structure ($\widehat{\text{sec}}$).

(4) Rotation at 19.78 sec-transient plus steady state vibration.

(5) Rotation at 19.78 sec-transient vibration almost zero.

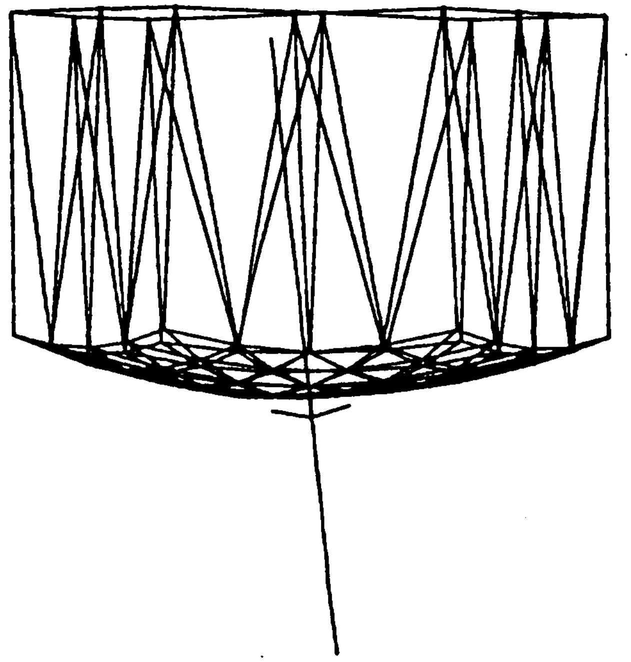

Figure 7. - JPL Configuration, Mode 7, 0.54 Hz

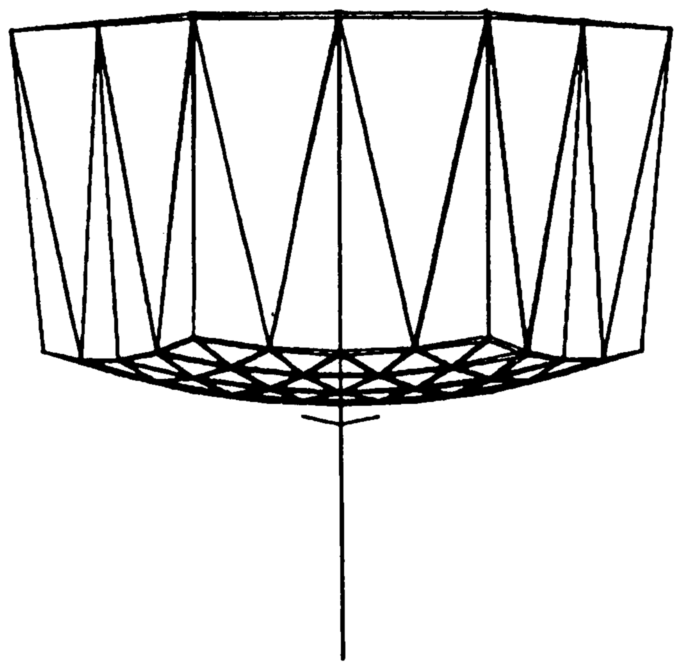

Figure 8. - JPL Configuration, Mode 9, 0.61 Hz

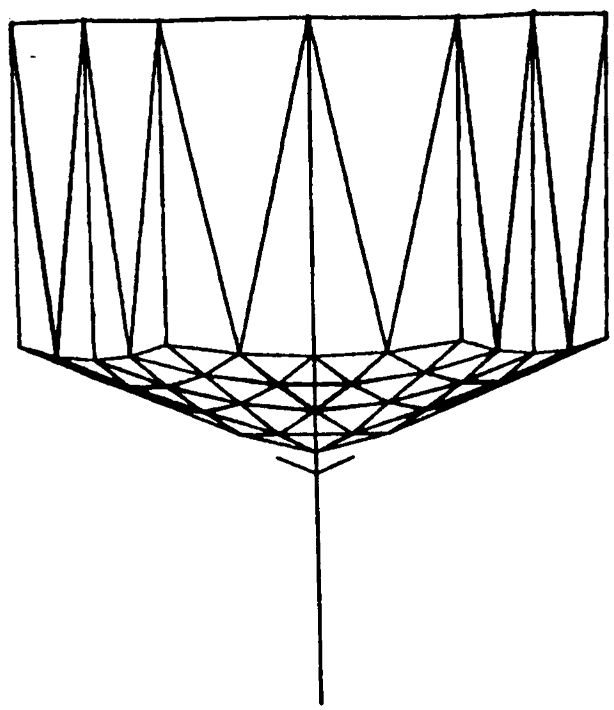

Figure 9. - JPL Configuration, Mode 12, 1.54 Hz

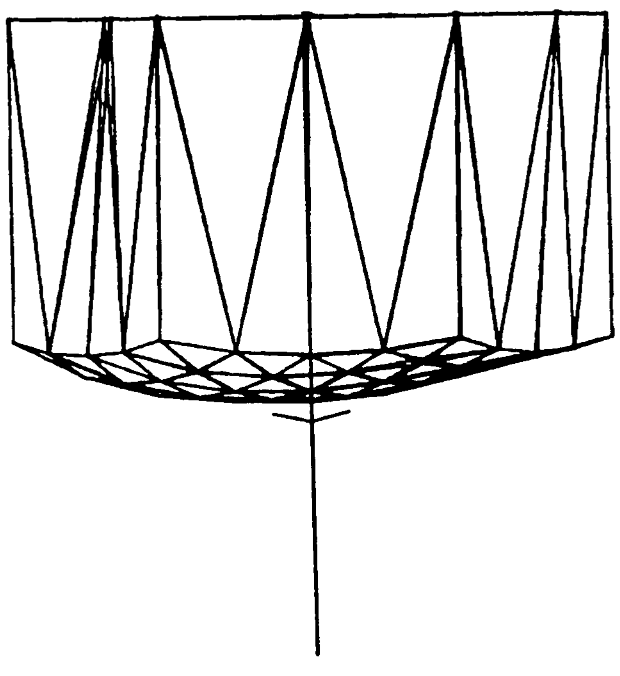

Figure 10. - JPL Configuration, Mode 16, 3.27 Hz

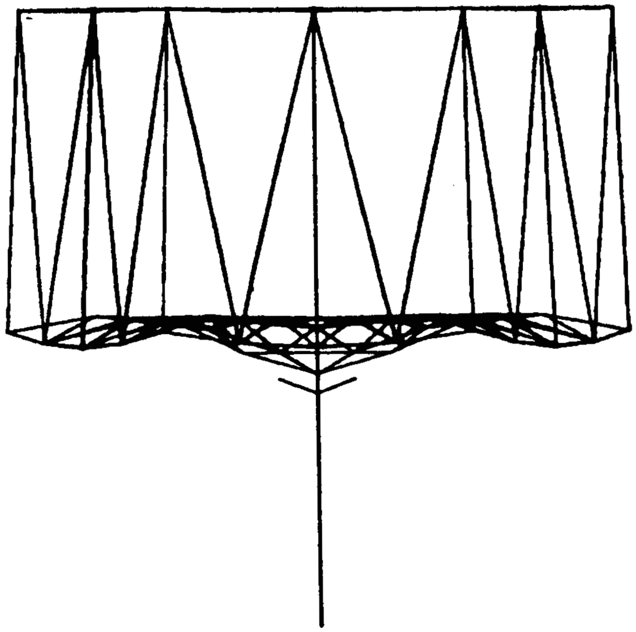

Figure 11. - JPL Configuration, Mode 18, 3.31 Hz

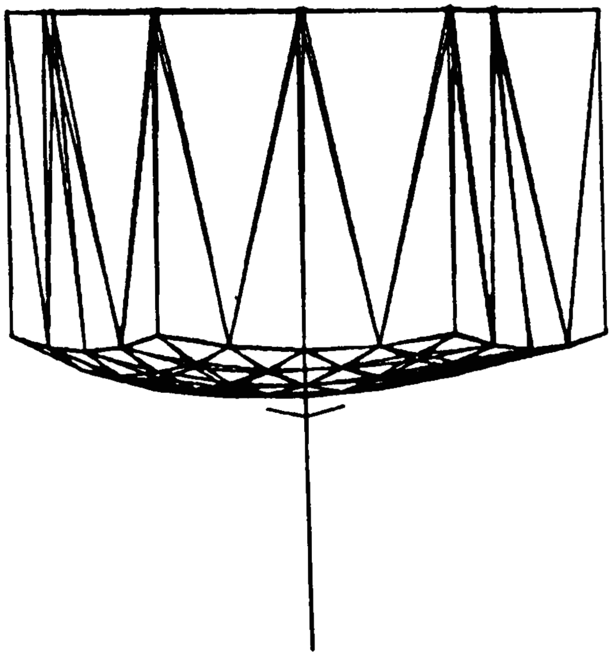

Figure 12. - JPL Configuration, Mode 20, 3.61 Hz

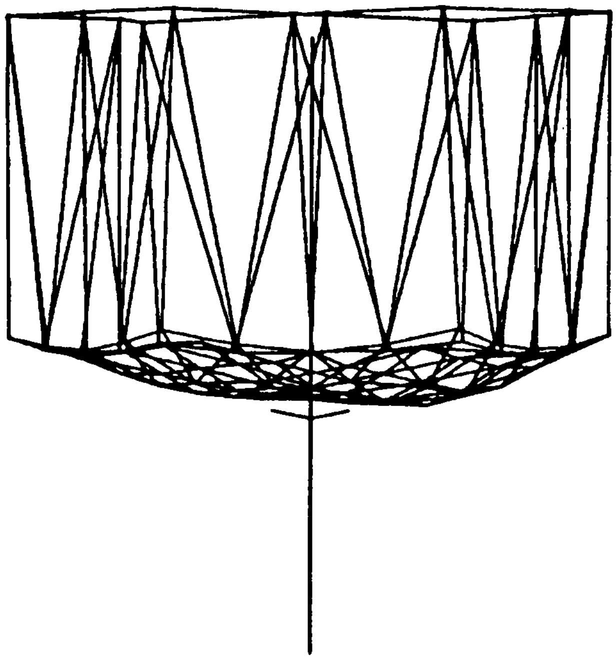

Figure 13. - JPL Configuration, Mode 21, 3.74 Hz

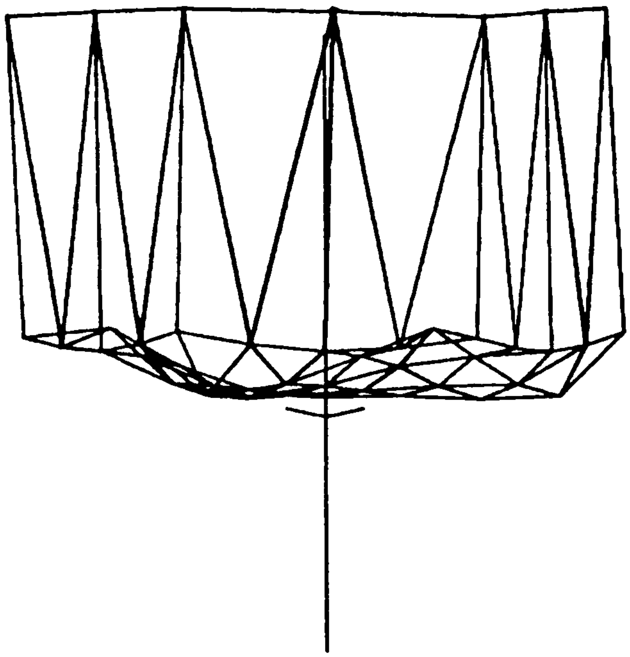

Figure 14. - JPL Configuration, Mode 24, 3.95 Hz

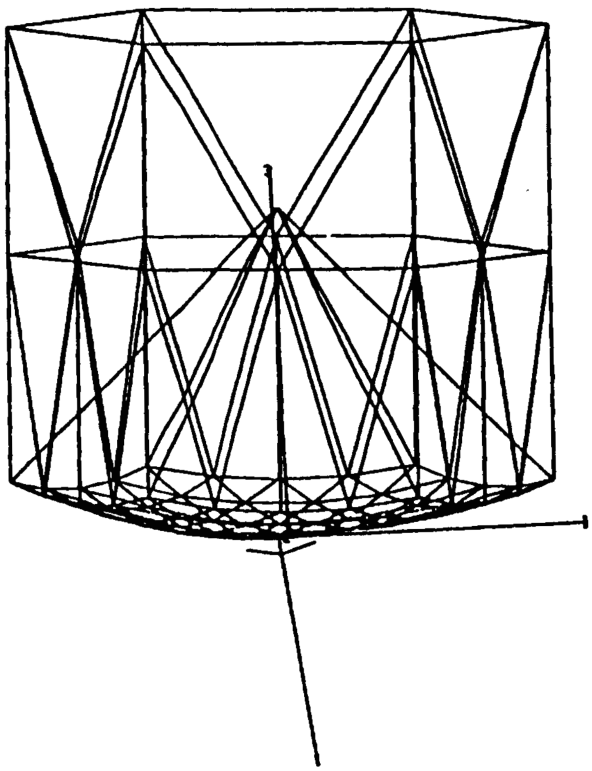

Figure 15. - Ames Six-Strut Configuration, Mode 7, 0.68 Hz

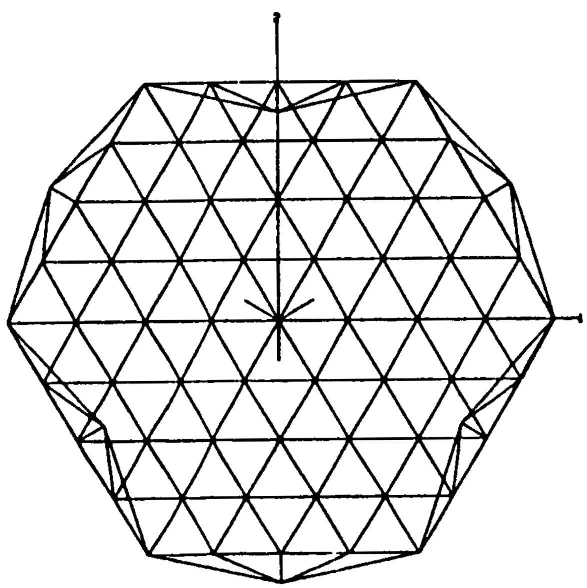

Figure 16. - Ames Six-Strut Configuration, Mode 9, 1.43 Hz

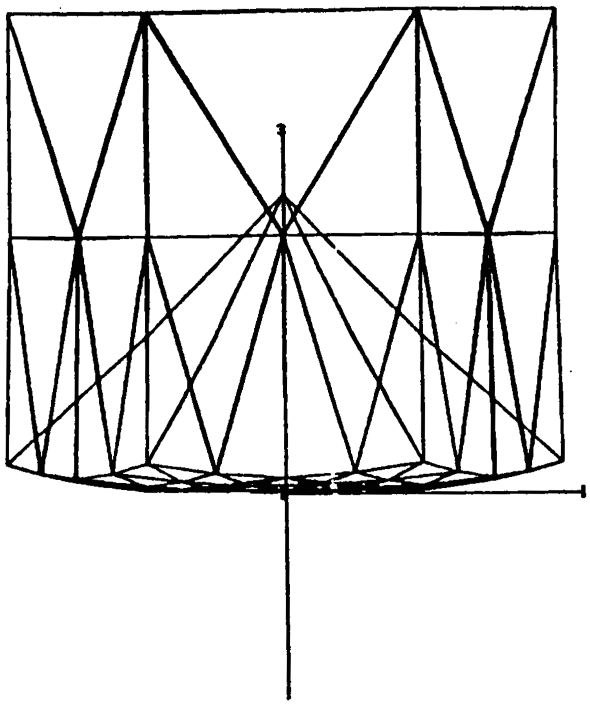

Figure 17. - Ames Six-Strut Configuration, Mode 10, 1.47 Hz

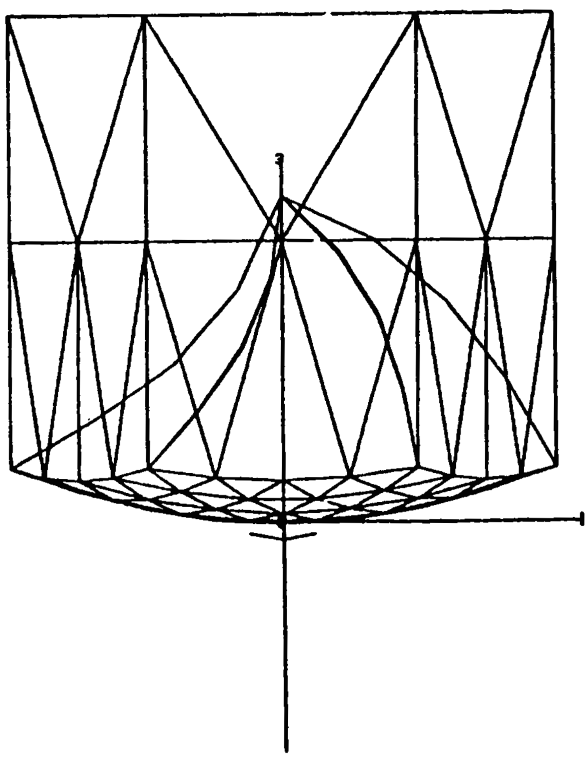

Figure 18. - Ames Six-Strut Configuration, Mode 11, 1.52 Hz

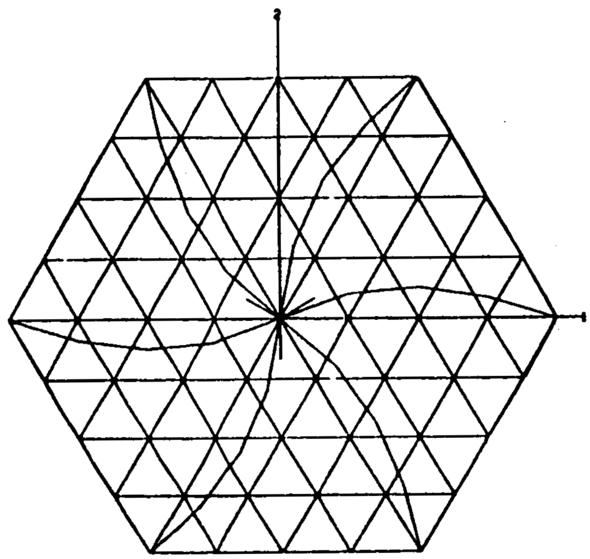

Figure 19. - Ames Six-Strut Configuration, Mode 15, 2.12 Hz

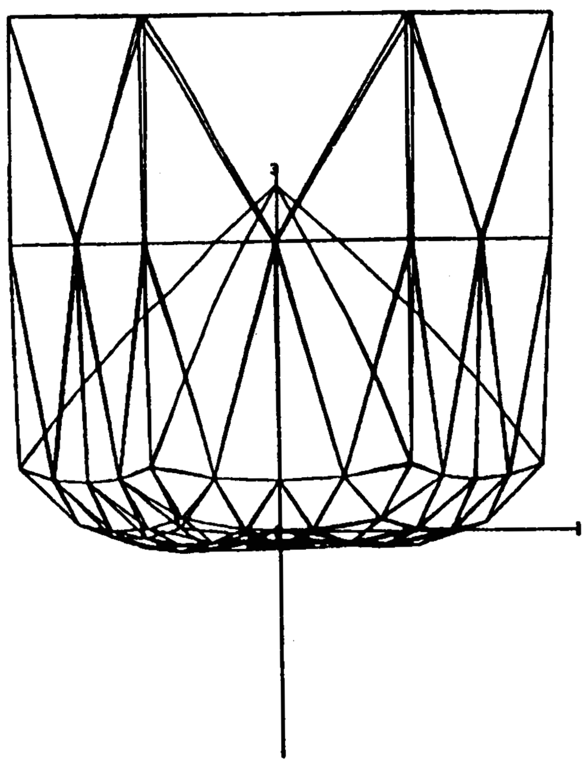

Figure 20. - Ames Six-Strut Configuration, Mode 22, 3.01 Hz

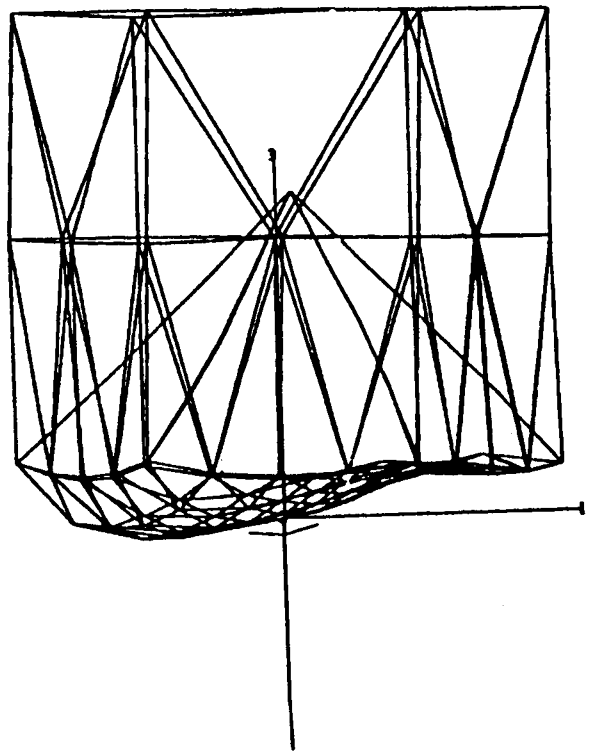

Figure 21. - Ames Six-Strut Configuration, Mode 24, 3.09 Hz

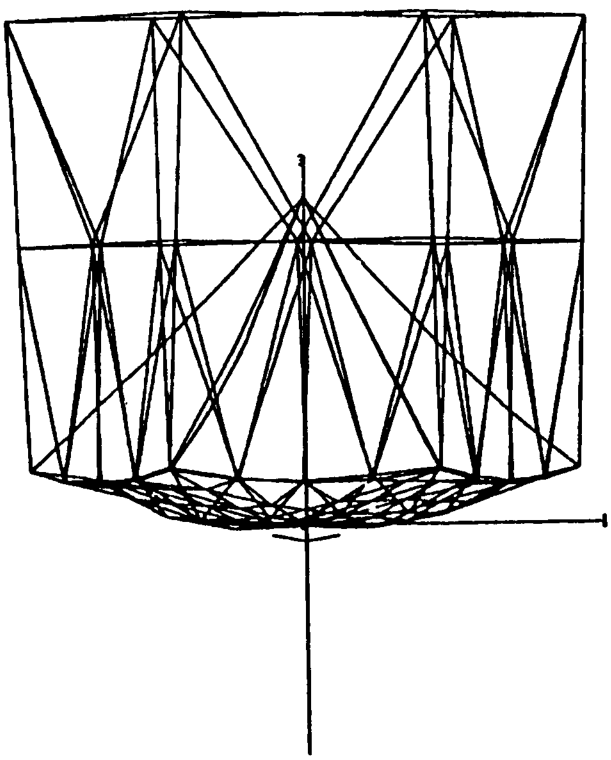

Figure 22. - Ames Six-Strut Configuration, Mode 25, 3.75 Hz

ORIGINAL PAGE IS
OF POOR QUALITY

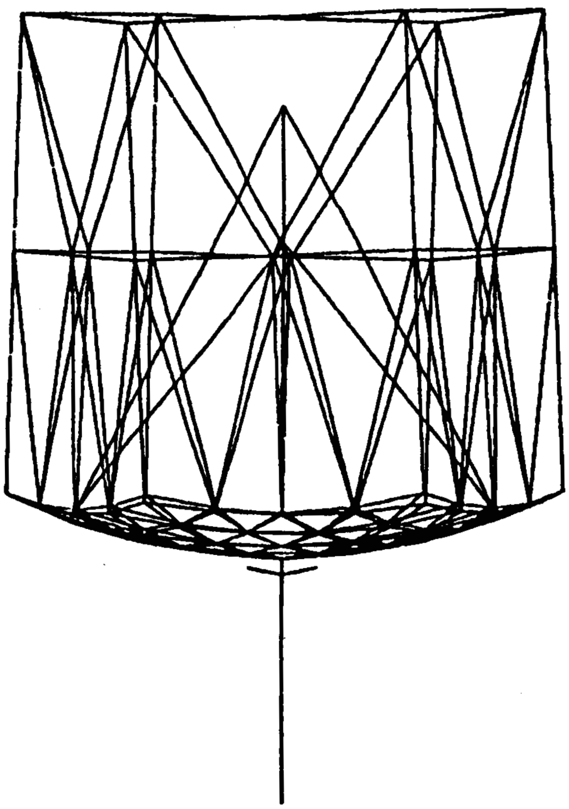

Figure 23. - Ames Triple-Bipod-Strut Configuration, Mode 7, 0.56 Hz

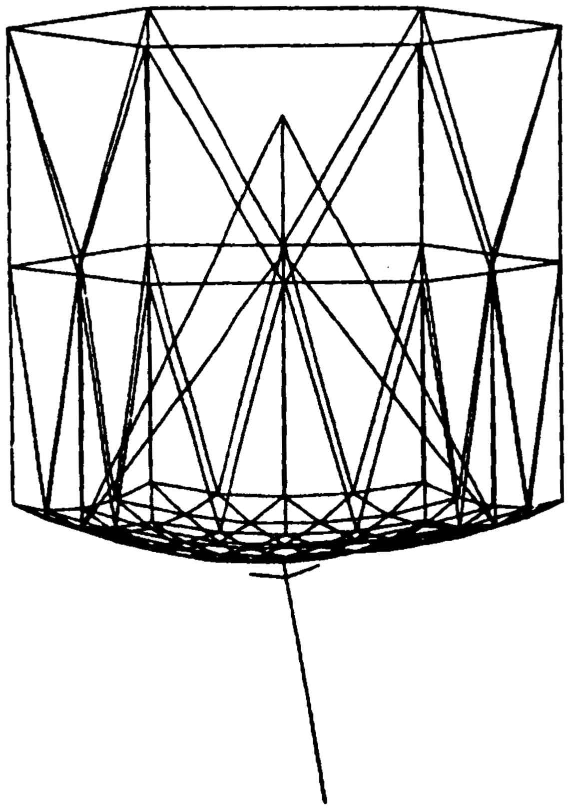

Figure 24. - Ames Triple-Bipod-Strut Configuration, Mode 9, 0.65 Hz

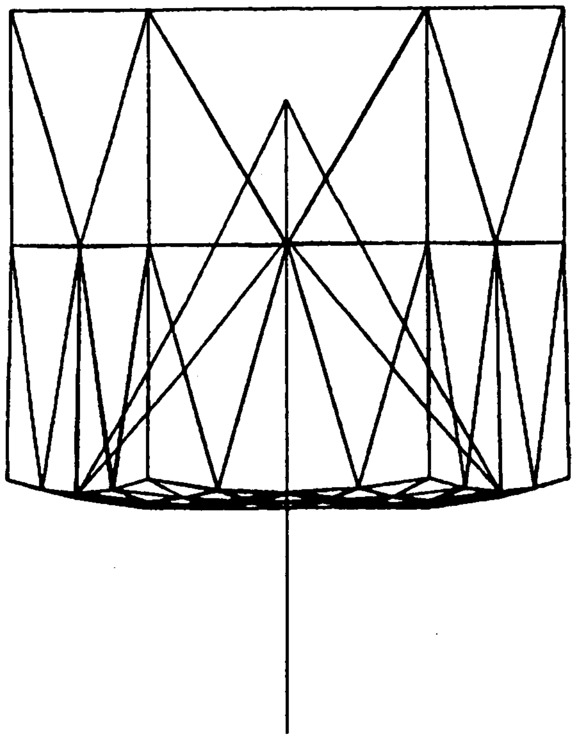

Figure 25. - Ames Triple-Bipod-Strut Configuration, Mode 13, 1.48 Hz

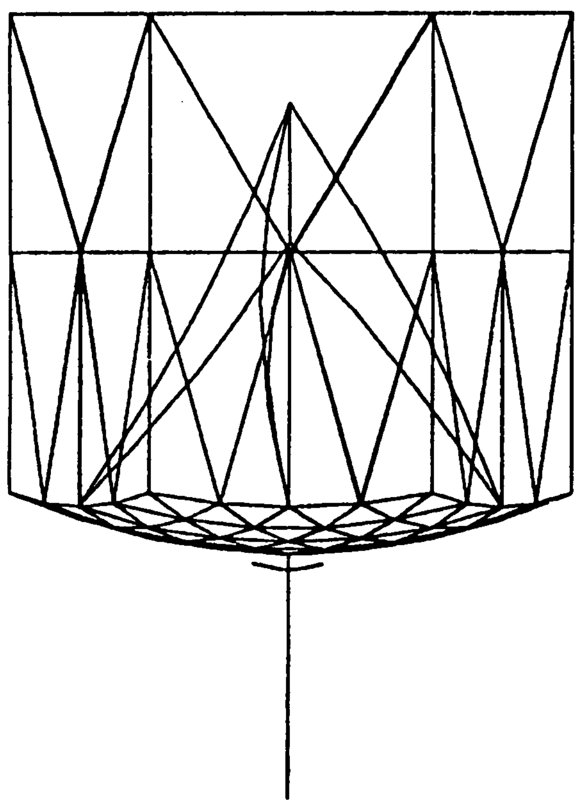

Figure 26. - Ames Triple-Bipod-Strut Configuration, Mode 16, 1.94 Hz

ORIGINAL PAGE IS
OF POOR QUALITY

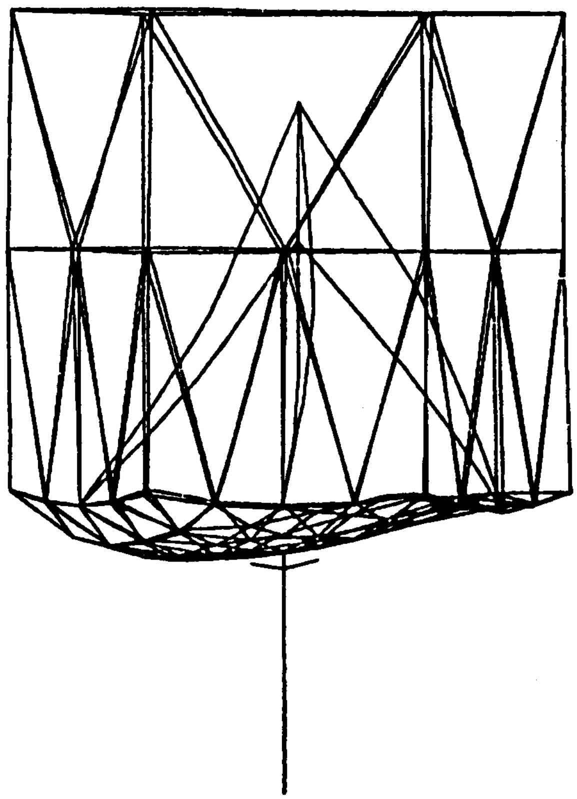

Figure 27. - Ames Triple-Bipod-Strut Configuration, Mode 21, 2.98 Hz

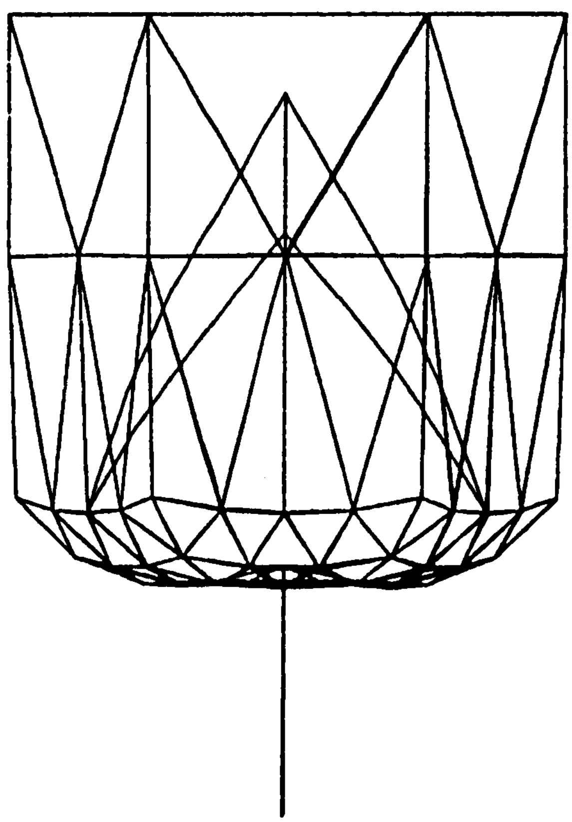

Figure 28. - Ames Triple-Bipod-Strut Configuration, Mode 22, 3.04 Hz

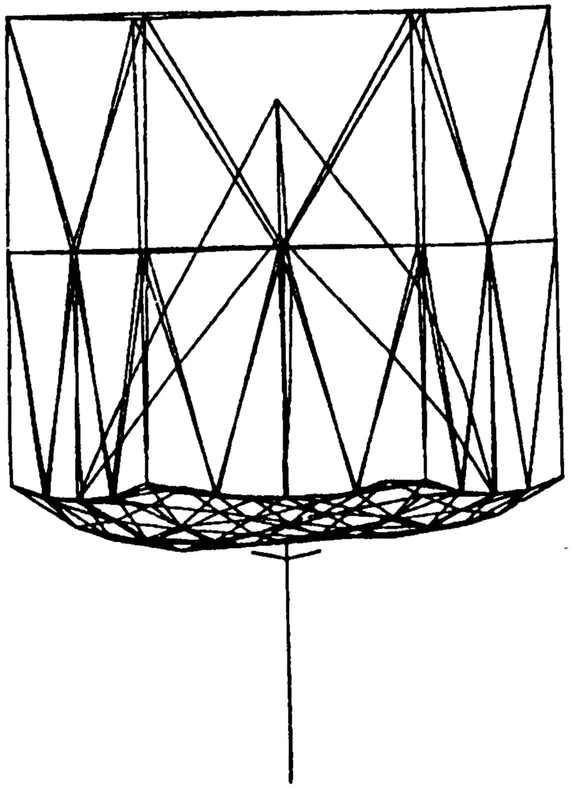

Figure 29. - Ames Triple-Bipod-Strut Configuration, Mode 24, 3.59 Hz

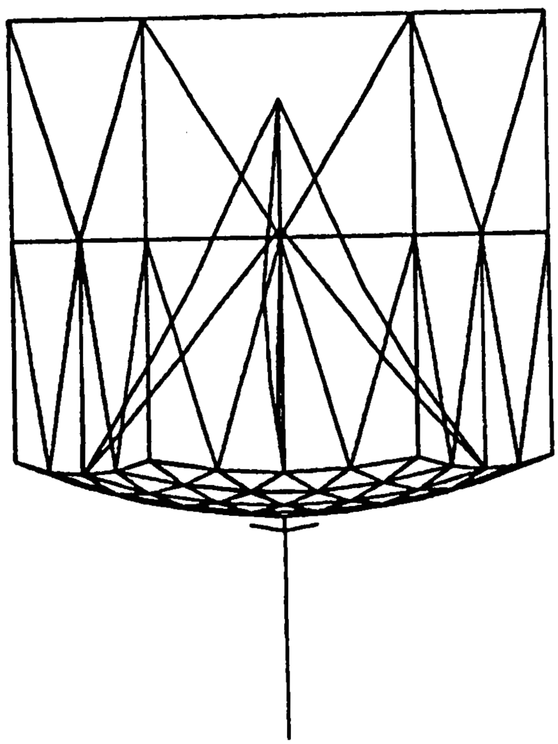

Figure 30. - Ames Triple-Bipod-Strut Configuration, Mode 25, 3.74 Hz

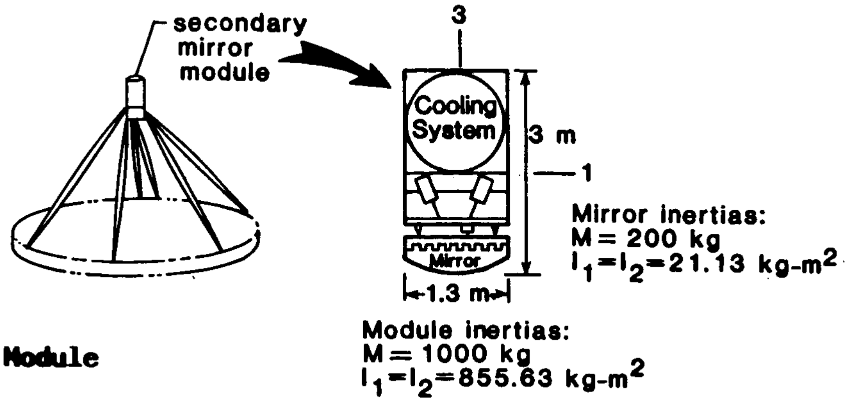

(a) Module

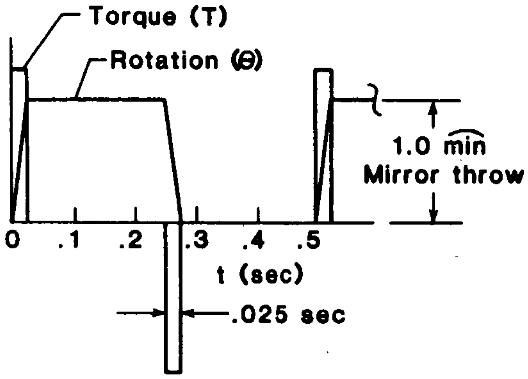

(b) Mirror Chopping Torque and Rotation

Figure 31. - Secondary Mirror Chopping

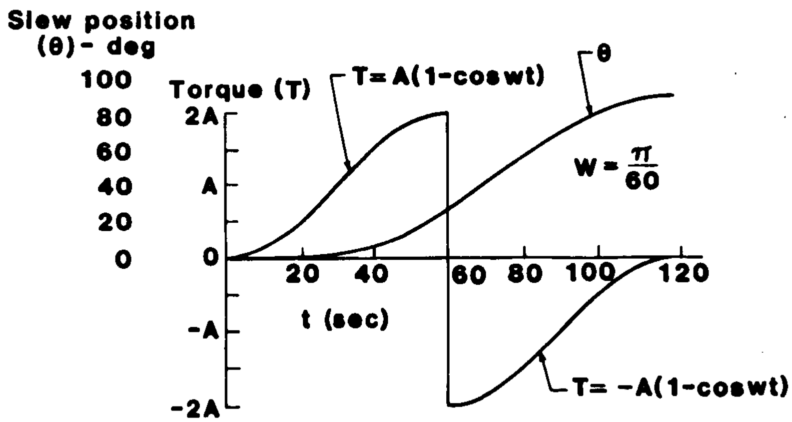

Configuration	T_{max} = 2A N-m (in-lb)
JPL	820 (7256)
Ames six strut	985 (8720)
Ames bipod strut	1008 (8918)

Figure 32. - LDR Slewing Torque and Position

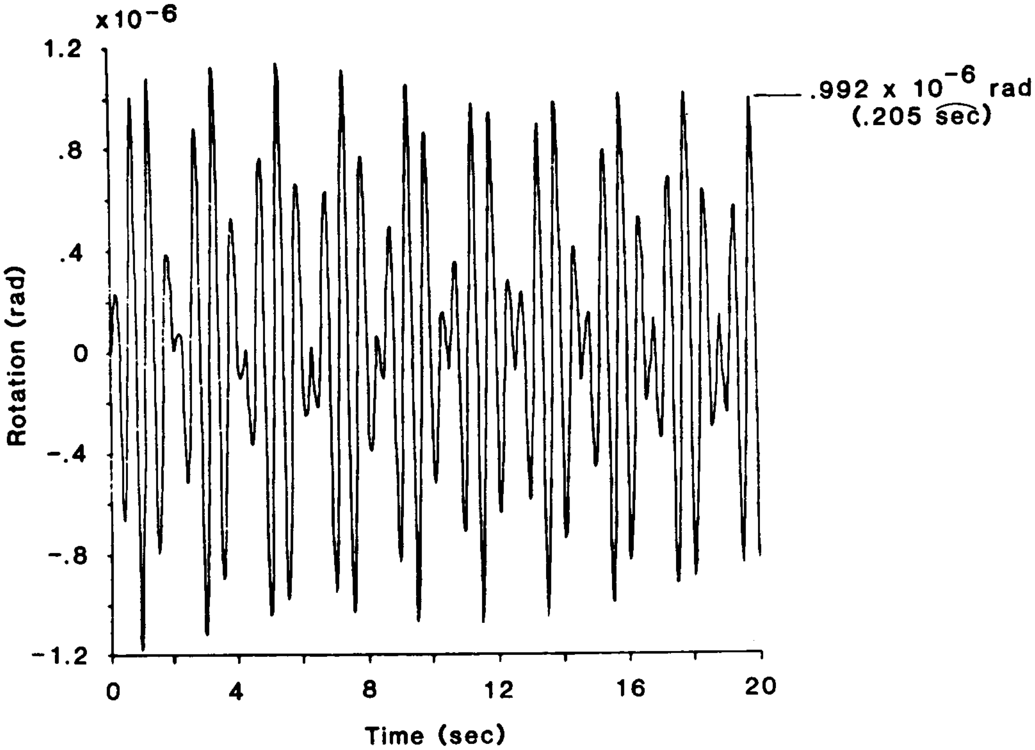

(a) 0.002 Damping Ratio

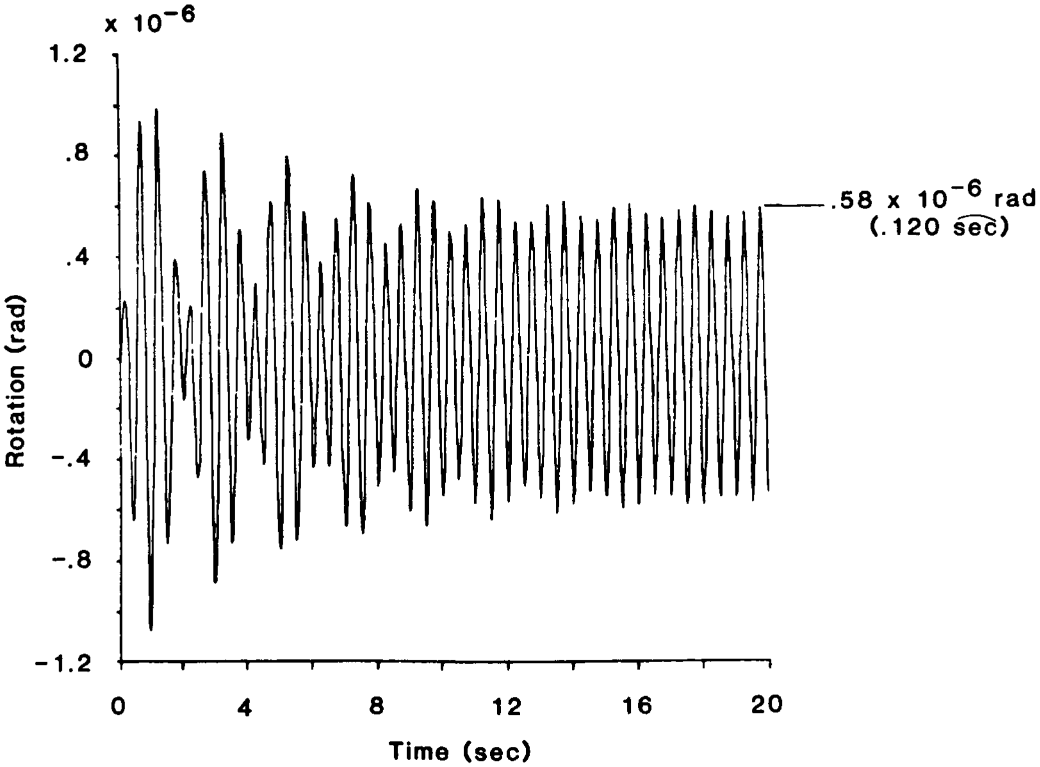

Figure 33. - Ames Six-Strut Secondary Mirror Module Jitter from Chopping

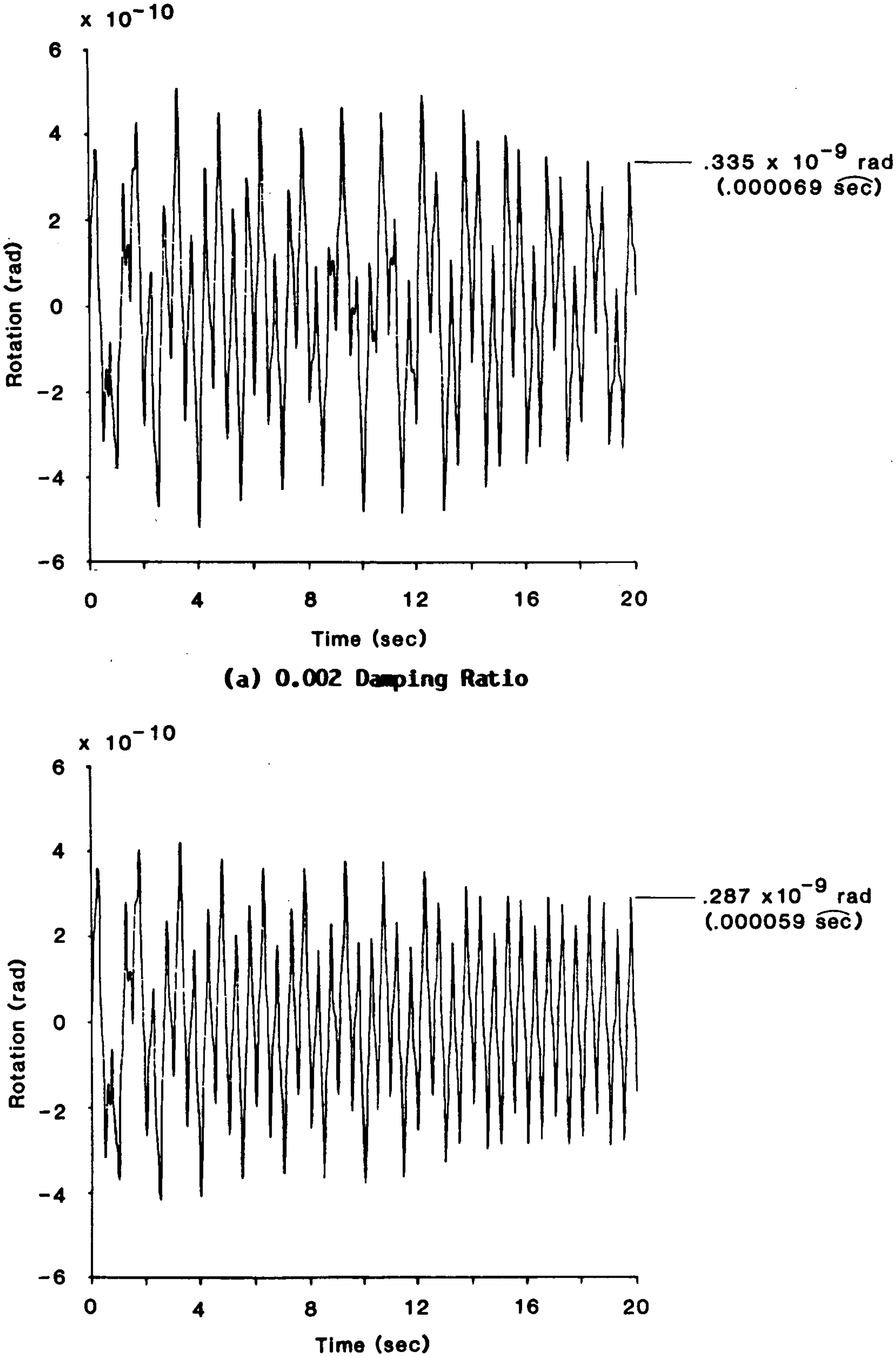

(a) 0.002 Damping Ratio

(b) 0.02 Damping Ratio

Figure 34. - Ames Triple-Bipod Strut Secondary Mirror Module Jitter from Chopping

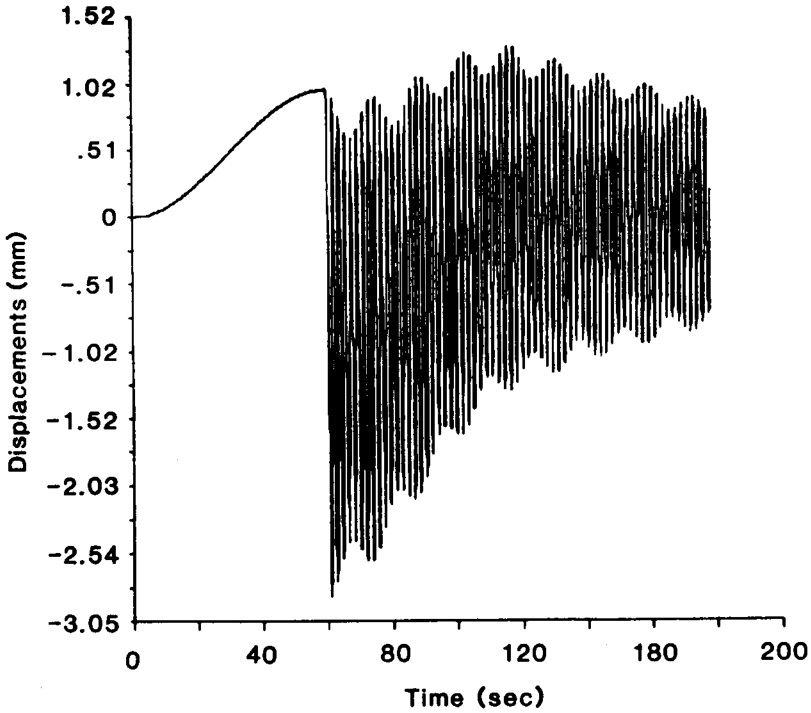

(a) 0.002 Damping Ratio

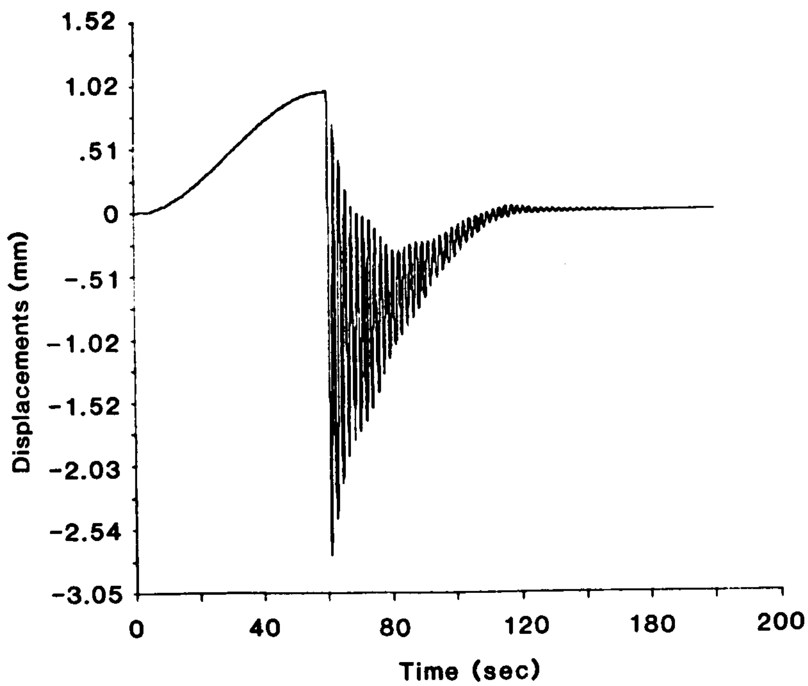

(b) 0.02 Damping Ratio

Figure 35. - JPL Reflector Jitter from Slew. Displacement at Reflector Truss/Shade Joint

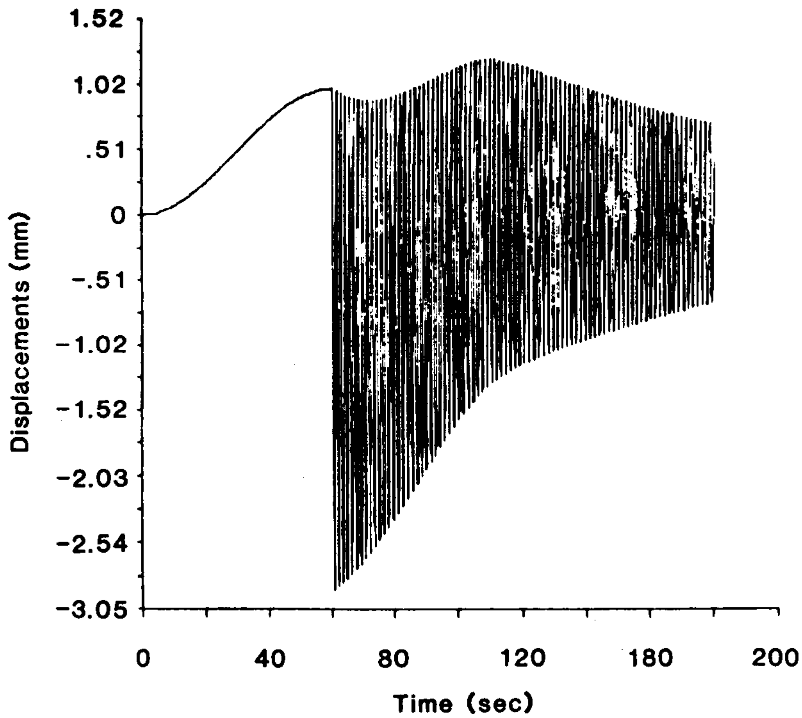

(a) 0.002 Damping Ratio

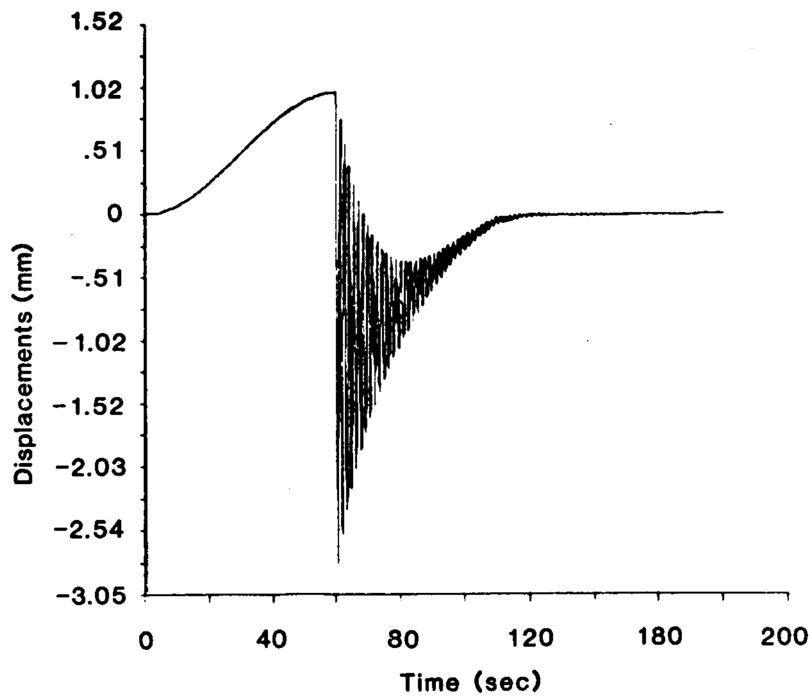

(b) 0.02 Damping Ratio

Figure 36. - Ames Six-Strut Reflector Jitter from Slew.
Displacement at Reflector Truss/Shade Joint

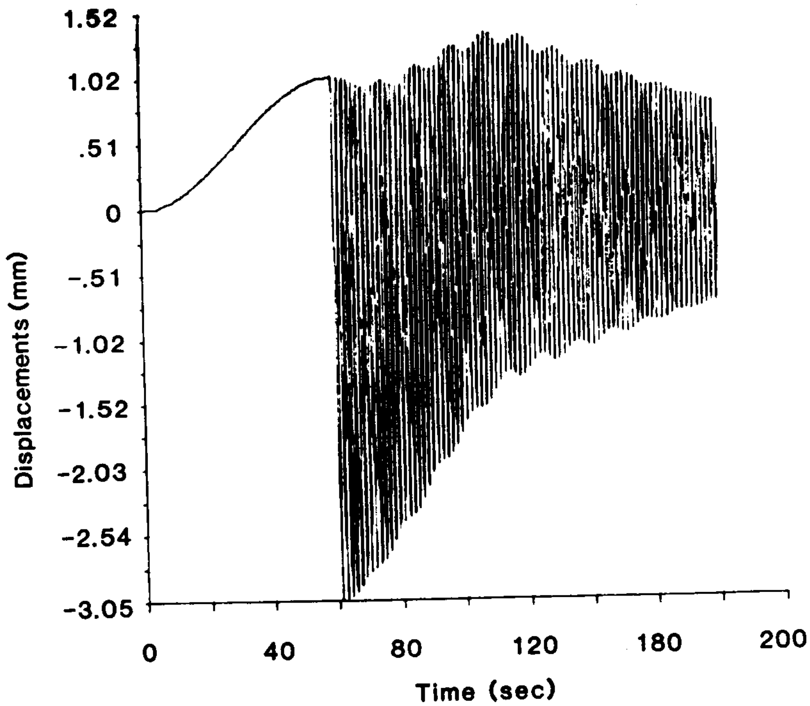

(a) 0.002 Damping Ratio

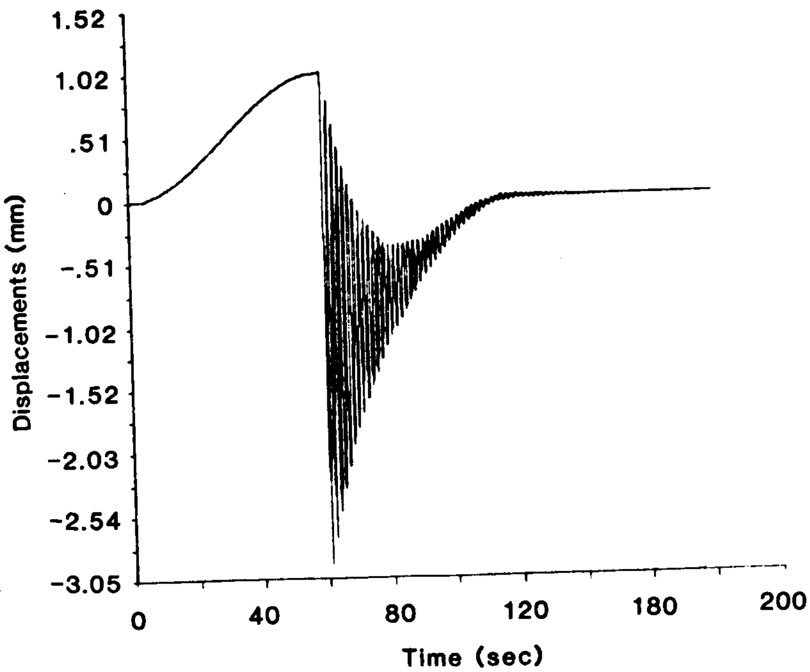

(b) 0.02 Damping Ratio

Figure 37. - Ames Triple-Bipod Strut Reflector Jitter from Slew. Displacement at Reflector Truss/Shade Joint

1. Report No.
NASA TM-89056

2. Government Accession No.

3. Recipient's Catalog No.

4. Title and Subtitle
Dynamic Analysis of the Large Deployable Reflector

5. Report Date
January 1987

6. Performing Organization Code
506-49-31-01

7. Author(s)
Robert E. Calleson
A. Don Scott

8. Performing Organization Report No.

9. Performing Organization Name and Address
NASA Langely Research Center
Hampton, VA 23665-5225

10. Work Unit No.

11. Contract or Grant No.

12. Sponsoring Agency Name and Address
National Aeronautics and Space Administration
Washington, DC 20546-0001

13. Type of Report and Period Covered
Technical Memorandum

14. Sponsoring Agency Code

15. Supplementary Notes
Robert E. Calleson, PRC Kentron, Inc., Hampton, Virginia.
A. Don Scott, NASA Langley Research Center, Hampton, Virginia.

16. Abstract
The Large Deployable Reflector (LDR) is to be an astronomical observatory orbiting above Earth's obscuring atmosphere and operating in the spectral range between 30 um and 1000 um wavelength. The LDR will be used to study such astronomical phenomena as stellar and galactic formation, cosmology, and planetary atmospheres. The LDR will be the first observatory to be erected and assembled in space. This distinction brings with it several major technological challenges such as the development of ultra-lightweight deployable mirrors, advanced mirror fabrication techniques, advanced structures, and control of vibrations due to various sources of excitation. The purpose of this analysis is to provide a assessment of the vibrational response due to secondary mirror chopping and LDR slewing. The dynamic response of two 20-m LDR configurations was studied. Two mirror support configurations were investigated for the Ames concept, the first employs a six-strut secondary mirror support structure, while the second uses a triple-bipod support design. All three configurations were modeled using a tetrahedral truss design for the primary mirror support structure. Response resulting from secondary mirror chopping was obtained for the two Ames configurations, and the response of the primary mirror from slewing was obtained for all three configurations.

17. Key Words (Suggested by Author(s))
Large Deployable Reflector
Primary Mirror
Secondary Mirror
Chopping
Slew
Response

18. Distribution Statement
Unclassified - Unlimited

Subject Category - 18

19. Security Classif. (of this report)
Unclassified

20. Security Classif. (of this page)
Unclassified

21. No. of Pages
33

22. Price
A03